BIOTECHNOLOGY

CRISPR-mediated live imaging of genome editing and transcription

Haifeng Wang[1], Muneaki Nakamura[1], Timothy R. Abbott[1], Dehua Zhao[1], Kaiwen Luo[1,2], Cordelia Yu[1,3], Cindy M. Nguyen[1], Albert Lo[1], Timothy P. Daley[1,4], Marie La Russa[1], Yanxia Liu[1], Lei S. Qi[1,5,6]*

We report a robust, versatile approach called CRISPR live-cell fluorescent in situ hybridization (LiveFISH) using fluorescent oligonucleotides for genome tracking in a broad range of cell types, including primary cells. An intrinsic stability switch of CRISPR guide RNAs enables LiveFISH to accurately detect chromosomal disorders such as Patau syndrome in prenatal amniotic fluid cells and track multiple loci in human T lymphocytes. In addition, LiveFISH tracks the real-time movement of DNA double-strand breaks induced by CRISPR-Cas9–mediated editing and consequent chromosome translocations. Finally, by combining Cas9 and Cas13 systems, LiveFISH allows for simultaneous visualization of genomic DNA and RNA transcripts in living cells. The LiveFISH approach enables real-time live imaging of DNA and RNA during genome editing, transcription, and rearrangements in single cells.

Genome editing can induce chromosomal rearrangements, including translocations (*1*, *2*). Although sequencing approaches have been used to identify and characterize chromosomal abnormalities associated with genetic disorders and gene editing, the temporal dynamics of chromosomal rearrangements are less well known. Previous studies relied on using genomic-integrated LacO/TetO arrays, which is a tedious and challenging method (*3*). Fluorescent protein-fused, nuclease-deactivated dCas9 or single guide RNA (sgRNA) recruiting fluorescent protein-fused RNA-binding proteins enable CRISPR-mediated live imaging of genomic loci (*4*–*7*). However, DNA-encoded CRISPR components are required, limiting its usage. Traditional fluorescent in situ hybridization (FISH) requires DNA denaturation, whereas fluorescent labeled-dCas9 assembled in vitro with sgRNA (CASFISH) detects genomic loci only in fixed samples, precluding real-time tracking (*8*, *9*). Here, we report a live-imaging approach, CRISPR LiveFISH, that allows for the real-time study of various chromosomal functions in living cells.

We first assembled equimolar amounts of dCas9-EGFP (enhanced green fluorescent protein) protein and Cy3-labeled guide RNA (gRNA) as fluorescent ribonucleoproteins (fRNPs), which target a repetitive region in chromosome 3 (Chr3q29, ~500 repeats) (*4*, *5*, *7*). We delivered fRNPs into human bone osteosarcoma U2OS cells by electroporation (Fig. 1A, fig. S1A, and table S1) (*10*). Flow cytometry analysis showed that >95% of gRNA signals were degraded within 4 hours after transfection (fig. S1B), consistent with previous reports showing that gRNAs are highly unstable in the cellular environment (*11*, *12*). However, we observed a rapid and long-lasting labeling of Cy3-gRNA at the Chr3 site, suggesting the

[1]Department of Bioengineering, Stanford University, Stanford, CA 94305, USA. [2]ZJU-UOE Institute, Zhejiang University, School of Medicine, Haining, China. [3]Castilleja School, Palo Alto, CA 94301, USA. [4]Department of Statistics, Stanford University, Stanford, CA 94305, USA. [5]Department of Chemical and Systems Biology, Stanford University, Stanford, CA 94305, USA. [6]ChEM-H Institute, Stanford University, Stanford, CA 94305, USA.
*Corresponding author. Email: stanley.qi@stanford.edu

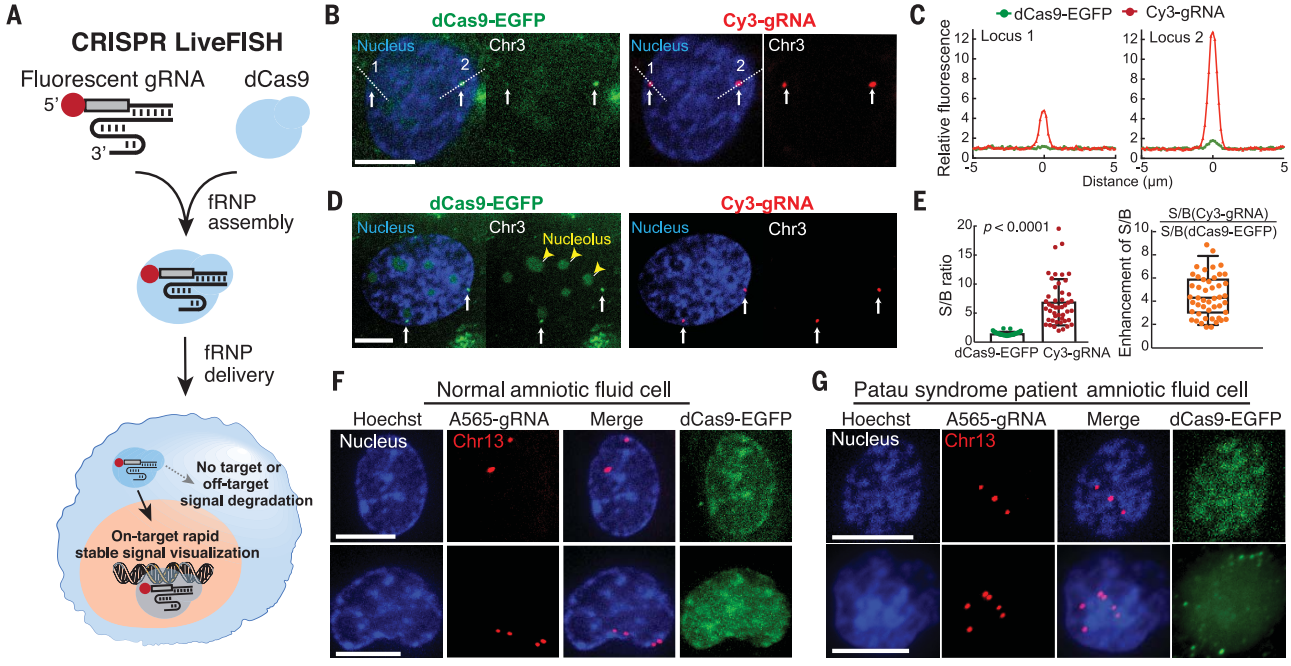

Fig. 1. DNA target–dependent protection of gRNA enables LiveFISH for robust genomic tracking and cytogenetic diagnosis in primary cells. (**A**) Schematic of LiveFISH for genomic imaging and cytogenetic detection in living cells by fluorescent ribonucleoprotein (fRNP) consisting of synthesized fluorescent gRNA and dCas9. (**B** to **D**) Comparison of fluorescent gRNA (Cy3-gRNA, red) and dCas9-EGFP (green) labeling of a repetitive Chr3q29 locus (white arrows) in U2OS cells by fRNP delivery. The dotted lines in (B) mark the area used to produce the line scan in (C). The yellow arrowheads in (D) show nucleolar dCas9-EGFP accumulation. (**E**) Comparison of signal-to-background ratio (S/B) of labeled Chr3q29 loci using fluorescent gRNA (red) and dCas9-EGFP (green). Left: mean ± SD, $p < 0.0001$ by Wilcoxon test; right: box plot of calculated ratios (orange) between the S/B of Cy3-gRNA and dCas9-EGFP at each locus. (**F** and **G**) Images of LiveFISH imaging and cytogenetic detection in normal (F) and Patau syndrome patient–derived (G) amniotic fluid cells with fRNP containing dCas9-EGFP (green) and Atto565-gRNA (red) targeting Chr13. See movies S1 and S2 for dynamics. Scale bars, 10 μm.

formation of a stable target-bound dCas9-gRNA complex (fig. S1C). The signal-to-background ratio (S/B) of gRNA was more than fourfold higher than that of dCas9-EGFP (Fig. 1, B to E, and fig. S1D). Unlike dCas9-EGFP, which frequently accumulated in the nucleolus, there was no nucleolar accumulation of gRNA (Fig. 1D). We performed in vitro assays and found that excessive target DNA, but not nontarget DNA, strongly protected gRNA within the Cas9:gRNA:DNA ternary complex from ribonuclease A (RNase A) degradation (fig. S2, A to C). In addition, dCas9-bound gRNA was better protected by fully matched target DNA or target DNA with ≤4-base pairs (bp) PAM (protospacer adjacent motif)-distal mismatches than target DNAs with ≥6-bp mismatches (fig. S2, D to G).

On the basis of this target DNA–dependent protection of gRNA, we developed CRISPR LiveFISH, an approach that deploys fluorescent gRNA probes assembled with dCas9 to target and label genomic sequences in living cells (Fig. 1A). We tested CRISPR LiveFISH on cells derived from patients with Patau syndrome, a Chr13 trisomy genetic disorder that results in organ defects and intellectual and physical impairment, and eventually patient death (*13*). We transfected fRNPs containing dCas9 and Atto565-labeled gRNA to target a repetitive Chr13 region (Chr13q34, ~350 repeats) into normal or patient-derived prenatal amniotic fluid cells and detected rapid and robust Chr13 labeling by Atto565-gRNA, which outperformed dCas9-EGFP RNP labeling or plasmid-based imaging (Fig. 1, F and G; fig. S3, A to D; and movies S1 and S2). The high efficiency of LiveFISH can be quantified, and its accuracy was confirmed by karyotyping (fig. S3, D and E, and fig. S4). Simple co-delivery of fRNPs labeled with different fluorophores enabled simultaneous visualization of repetitive Chr3 and Chr13 regions in U2OS cells (fig. S5A) and in primary human T lymphocytes (fig. S5B and movie S3). Previous methods using orthogonal dCas9s (*6*, *14*) or coupling sgRNAs to RNA aptamers and RNA-binding proteins (*7*) instead require multiple constructs.

We next applied LiveFISH to study the real-time dynamics of CRISPR-Cas9–induced DNA double-strand breaks (DSBs) in living cells. We created a U2OS cell line that stably expressed a

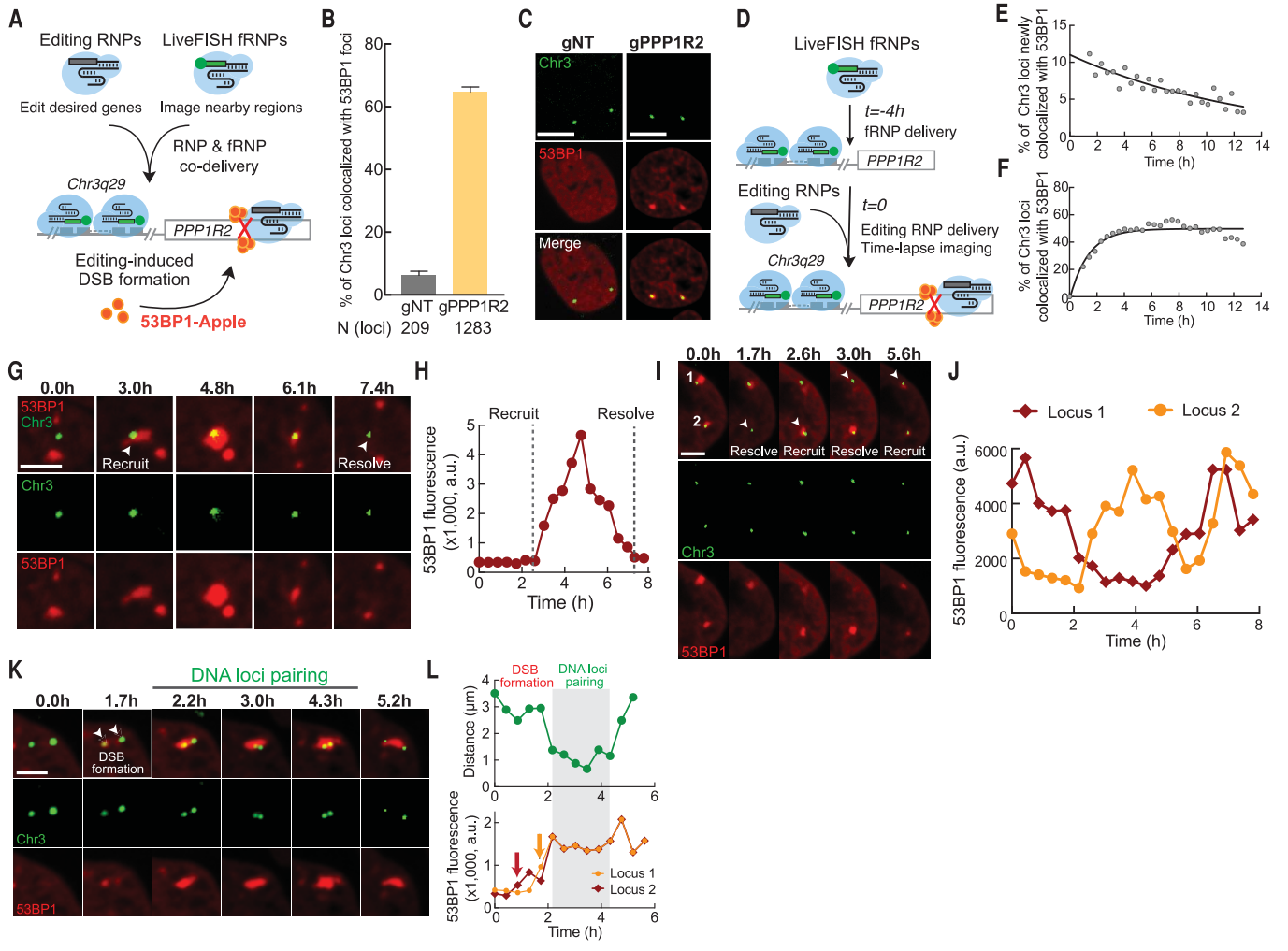

Fig. 2. LiveFISH real-time visualization of gene-editing–induced DNA DSBs in living cells. (**A**) Schematic depicting visualization of gene-editing–induced DSB dynamics by co-delivering LiveFISH fRNPs and CRISPR editing RNPs in 53BP1-Apple U2OS cells. (**B**) Percentages of 53BP1-colocalized Chr3 loci using a nontargeting gRNA (gNT) and a *PPP1R2*-targeting gRNA (gPPP1R2). Data show mean ± SEM. $p < 0.0001$ by Fisher's exact test. (**C**) Representative images comparing localization of 53BP1 and Chr3 loci in cells with gNT and gPPP1R2. Scale bars, 10 μm. (**D**) Schematic depicting visualization of gene-editing–induced DSB dynamics by sequentially delivering LiveFISH fRNPs ($t = -4$ hours) and editing RNPs ($t = 0$). (**E** and **F**) Percentages of newly (E) and total (F) 53BP1-colocalized Chr3q29 loci over time after editing RNP delivery ($t = 0$). Black lines show nonlinear fits. (**G** and **H**) Representative images (G) and quantification of 53BP1 fluorescence (H) at Chr3q29 loci during gene editing. (**I** and **J**) Representative images (I) and quantification of 53BP1 fluorescence (J) during repeated recruitment and resolution of 53BP1 at Chr3q29 loci. (**K** and **L**) Representative images (K) and quantification of distance between the Chr3 loci [(L), top] and 53BP1 fluorescence [(L), bottom] during 53BP1 loci fusion and homologous Chr3 loci pairing. Colored arrows in (L) indicate 53BP1 foci formation. White arrowheads in (G), (I), and (K) show 53BP1-recruiting or -resolving events; a.u., arbitrary unit. Scale bars in (G), (I), and (K), 5 μm.

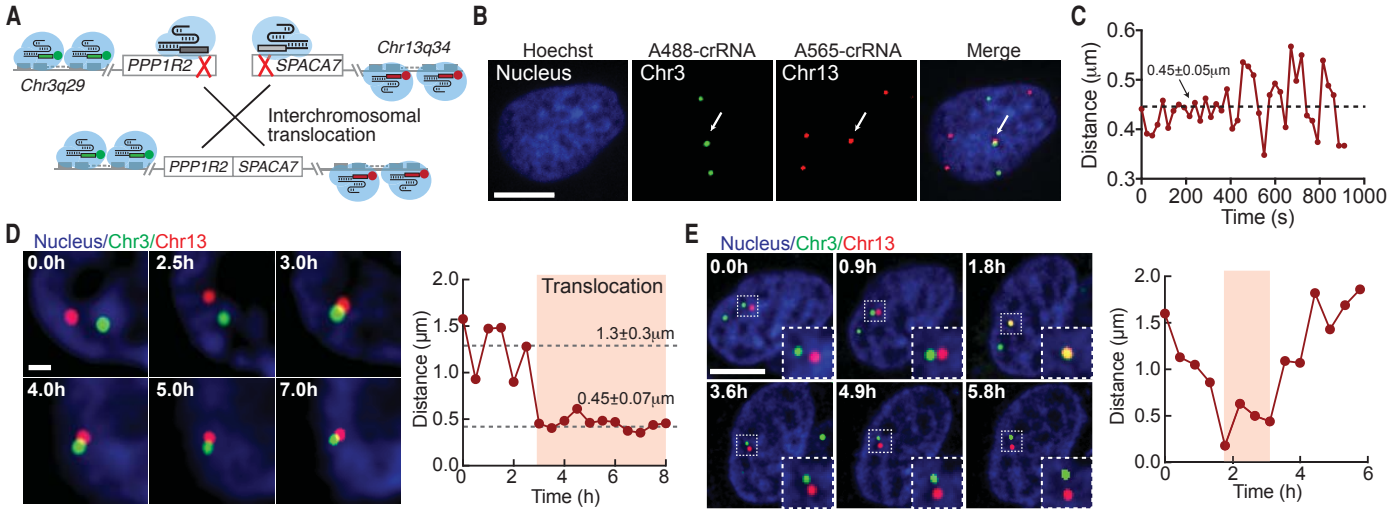

Fig. 3. LiveFISH detection and visualization of gene-editing–induced chromosome translocations in living cells. (**A**) Schematic depicting visualization of chromosomal translocations using LiveFISH fRNPs and CRISPR editing RNPs. (**B** and **C**) A representative U2OS cell (B) showing a pair of colocalized Chr3/Chr13 loci (arrow) and quantification of the Chr3/Chr13 distance (C) over a short time. See movie S4 for dynamics. Scale bar, 10 μm. (**D**) Representative images showing chromosomal translocation formation between Chr13 and Chr3 and distance over time. See movie S5 for dynamics. Scale bar, 1 μm. (**E**) Representative images showing transient colocalization between Chr13/Chr3 (outlined in white boxes) and distance over time. Scale bar, 10 μm.

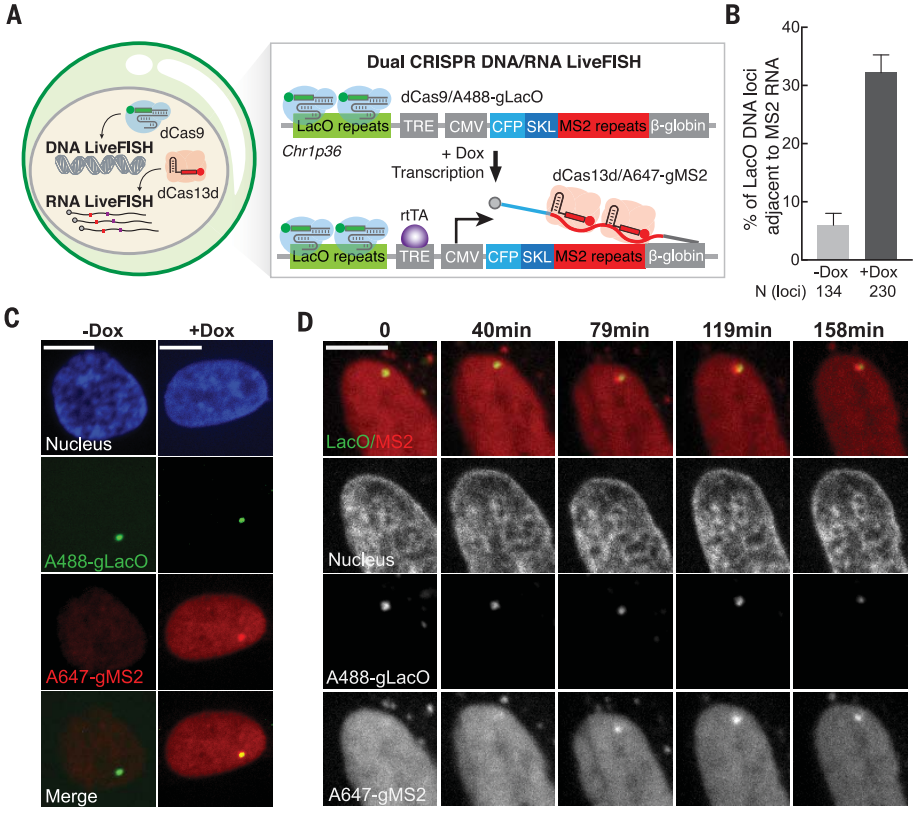

Fig. 4. Dual CRISPR DNA/RNA LiveFISH enables real-time visualization of transcription in living cells. (**A**) Schematic of dual DNA/RNA LiveFISH in living cells. (**B** and **C**) Percentages of LacO DNA loci showing adjacent labeled MS2 RNA with (+) or without (−) Dox (B) and representative images (C). (**D**) Representative images showing MS2 RNA transcription dynamics after adding a high concentration of Dox. Scale bars, 10 μm.

truncated 53BP1 protein (amino acids 1220 to 1711), a well-characterized DNA DSB sensor, fused with a fluorescent Apple protein. (*15*, *16*). The human genome contains repetitive sequences that are often adjacent (<100 kb) to most (>60%) protein-encoding genes (*17*). We co-delivered editing RNPs (Cas9/gPPP1R2) that cut the *PPP1R2* gene on Chr3 and LiveFISH fRNPs (Cas9/A488-gChr3) that labeled the repetitive Chr3q29 region, 36 kb from the *PPP1R2* cut site, into the U2OS-53BP1-Apple cells by nucleofection (Fig. 2A and table S2). To avoid fRNP-mediated DNA cutting, we used a short (11 nucleotide) spacer for the imaging gRNA, which is insufficient for DNA cleavage (*7*, *18*). After nucleofection, we observed that a high percentage of Chr3q29 loci colocalized with 53BP1 foci in cells containing the editing gRNA (Fig. 2, B and C), indicating rapid Cas9-induced DSB formation at the *PPP1R2* loci. Sequential delivery of imaging fRNPs and editing RNPs enabled us to track the process of DSB formation and 53BP1 recruitment at individual loci over time (Fig. 2D). After editing RNP delivery, we captured rapid and ongoing recruitment of 53BP1 foci to Chr3q29 loci that persisted for hours (Fig. 2, E and F, and table S3).

We were able to track the dynamics of gene-editing events. For example, we observed recruitment and subsequent dissociation of 53BP1 foci to the Chr3q29 locus, likely suggesting successful repair of DSBs (Fig. 2, G and H, and fig. S6A). We also observed repeated recruitment and resolution of 53BP1 foci at a single DNA locus in many cells, suggesting repeated cutting and repairing of the target DNA (Fig. 2, I and J, and fig. S6B). Finally, multiple Chr3q29 loci clustered within the same 53BP1 foci after editing RNP delivery

in some cells, indicating homologous pairing between the DSB loci as reported previously (*19*) (Fig. 2, K and L, and fig. S6, C and D). Two small 53BP1 bodies that initially formed at separate Chr3q29 loci rapidly fused together, and correspondingly the homologous Chr3q29 loci got closer inside the fused 53BP1 body, suggesting that fusion of 53BP1 bodies might facilitate homologous DSB loci pairing (Fig. 2, K and L, and fig. S6, C and D).

Using CRISPR to edit multiple genes is important for gene therapy (*20*, *21*), but can induce harmful nonhomologous chromosomal rearrangements (*1*, *2*). To visualize chromosomal translocations, we co-delivered editing RNPs targeting *PPP1R2* on Chr3 and *SPACA7* on Chr13, and LiveFISH fRNPs to track both Chr3q29 and Chr13q34 (82 kb from the *SPACA7* cutting site) (Fig. 3A, fig. S7A, and table S2). DSB formation at targeted loci was confirmed by 53BP1 immunostaining in U2OS cells (fig. S7B), which are often aneuploid (*22*). We were able to observe the pairing of Chr3q29 and Chr13q34 loci. The two loci showed almost identical movement trajectories (movie S4) and their distance remained almost constant (Fig. 3, B and C), suggesting a possible physical link between both loci. We tracked the translocation dynamics. Chr3q29 and Chr13q34 were initially separated, subsequently moved closer, and stayed together for a long period of time (Fig. 3D; fig. S8, A and B; and movie S5), likely representing endogenous nonhomologous chromosomal translocation. We also captured transient events, wherein Chr3q29 and Chr13q34 loci moved together briefly and separated (Fig. 3E and fig. S8C). To independently confirm chromosomal translocation, we cloned, sequenced, and verified the translocated segments (fig. S9).

We further expanded CRISPR LiveFISH to image both DNA and RNA in real time. We harnessed the catalytically deactivated Cas13d (CasRx), dCas13d, and synthesized fluorescent gRNAs for target RNA imaging (*23*). The U2OS 2-6-3 cell line harbors a repetitive LacO array upstream of a doxycycline (Dox)–inducible gene cassette containing an array of MS2 repeats (*24*) (Fig. 4A). To simultaneously visualize both DNA and RNA, we designed Atto488-labeled Cas9 gRNA to target LacO DNA (gLacO) and Atto647-labeled Cas13d gRNA to target MS2 RNA (gMS2). By co-delivery of gMS2 and dCas9/gLacO into U2OS 2-6-3 cells expressing dCas13d, we successfully labeled both DNA locus and RNA transcripts in the presence of Dox (Fig. 4, B and C). CRISPR LiveFISH also enabled us to track real-time dynamics of RNA transcription in living cells. We observed gradual accumulation of MS2 transcripts around the LacO locus over time after inducing transcription with a high concentration of Dox (Fig. 4D and fig. S10).

Here, we report the CRISPR LiveFISH technology for live-cell DNA and RNA imaging. Chemically synthesized fluorescent gRNAs in complex with dCas proteins can facilitate rapid, robust, and scalable genomic DNA tracking and RNA imaging in living cells, including primary cells (fig. S11 and table S4). The target DNA–dependent protection of gRNAs within the Cas9:gRNA:DNA ternary complex in the RNase-rich environment enriches target signals while minimizing background noise. LiveFISH also allows for dynamic tracking of CRISPR-induced gene editing and translocation events at endogenous genomic loci in living cells. Dual DNA-RNA CRISPR LiveFISH using both dCas9 and dCas13 systems enables live imaging of genomic DNA and RNA transcripts in the same cells. It is possible to combine CRISPR LiveFISH with other genetic manipulation technologies (e.g., CRISPRi/a, epigenetic modifications, and CRISPR-GO) to deepen our understanding of the spatiotemporal dynamics of genome organization and nuclear events (*5*, *17*, *25*, *26*).

REFERENCES AND NOTES

1. P. S. Choi, M. Meyerson, *Nat. Commun.* **5**, 3728 (2014).
2. M. Kosicki, K. Tomberg, A. Bradley, *Nat. Biotechnol.* **36**, 765–771 (2018).
3. V. Roukos *et al.*, *Science* **341**, 660–664 (2013).
4. M. Jinek *et al.*, *Science* **337**, 816–821 (2012).
5. B. Chen *et al.*, *Cell* **155**, 1479–1491 (2013).
6. H. Ma *et al.*, *Proc. Natl. Acad. Sci. U.S.A.* **112**, 3002–3007 (2015).
7. H. Ma *et al.*, *Nat. Biotechnol.* **34**, 528–530 (2016).
8. P. R. Langer-Safer, M. Levine, D. C. Ward, *Proc. Natl. Acad. Sci. U.S.A.* **79**, 4381–4385 (1982).
9. W. Deng, X. Shi, R. Tjian, T. Lionnet, R. H. Singer, *Proc. Natl. Acad. Sci. U.S.A.* **112**, 11870–11875 (2015).
10. X. Liang *et al.*, *J. Biotechnol.* **208**, 44–53 (2015).
11. H. Ma *et al.*, *J. Cell Biol.* **214**, 529–537 (2016).
12. A. Hendel *et al.*, *Nat. Biotechnol.* **33**, 985–989 (2015).
13. B. J. Baty, B. L. Blackburn, J. C. Carey, *Am. J. Med. Genet.* **49**, 175–188 (1994).
14. B. Chen *et al.*, *Nucleic Acids Res.* **44**, e75 (2016).
15. K. S. Yang, R. H. Kohler, M. Landon, R. Giedt, R. Weissleder, *Sci. Rep.* **5**, 10129 (2015).
16. Y. Huyen *et al.*, *Nature* **432**, 406–411 (2004).
17. H. Wang *et al.*, *Cell* **175**, 1405–1417.e14 (2018).
18. H. K. Liao *et al.*, *Cell* **171**, 1495–1507.e15 (2017).
19. M. Gandhi *et al.*, *Proc. Natl. Acad. Sci. U.S.A.* **109**, 9454–9459 (2012).
20. J. Ren *et al.*, *Oncotarget* **8**, 17002–17011 (2017).
21. S. Mattapally *et al.*, *J. Am. Heart Assoc.* **7**, e010239 (2018).
22. K. Al-Romaih *et al.*, *Cancer Genet. Cytogenet.* **144**, 91–99 (2003).
23. S. Konermann *et al.*, *Cell* **173**, 665–676.e14 (2018).
24. S. M. Janicki *et al.*, *Cell* **116**, 683–698 (2004).
25. L. S. Qi *et al.*, *Cell* **152**, 1173–1183 (2013).
26. I. B. Hilton *et al.*, *Nat. Biotechnol.* **33**, 510–517 (2015).

ACKNOWLEDGMENTS

We thank Stanford Cytogenetics Laboratory for karyotyping, Stanford Shared FACS Facilities for cell sorting, the Cell Sciences Imaging Facility and C. Espenel for microscope usage, ChEM-H Macromolecular Structure Knowledge Center for protein purification, D. L. Spector (Cold Spring Harbor Laboratory) for U2OS 2-6-3 cells, and Coriell Cell Repositories for amniotic fluid cell samples. **Funding**: T.R.A. acknowledges support from NSF GRFP. L.S.Q acknowledges funding support from the Li Ka Shing Foundation. This work is partly supported by the National Institutes of Health Common Fund 4D Nucleome Program (U01 EB021240), the Pew Scholar Foundation, and the Alfred P. Sloan Foundation. **Author contributions:** H.W. and L.S.Q. conceived the study. H.W. and L.S.Q. designed the experiments. H.W., M.N., T.R.A., D.Z., K.L., C.Y., C.M.N., A.L., and Y.L. performed the experiments. H.W., K.L., C.M.N., T.P.D., and L.S.Q. analyzed the data. H.W., M.L. and L.S.Q wrote the manuscript with help from all authors. **Competing interests:** H.W. and L.S.Q. are co-inventors of a patent filed by Stanford University on related work (U.S. provisional patent no. 29/393,761, 62/895,843). **Data and materials availability:** All data are available in the manuscript or the supplementary materials. Plasmids are available on Addgene.

SUPPLEMENTARY MATERIALS

science.sciencemag.org/365/6459/1301/suppl/DC1
Materials and Methods
Figs. S1 to S11
Tables S1 to S4
References (*27*–*31*)
Movies S1 to S5

22 April 2019; accepted 19 August 2019
Published online 5 September 2019
10.1126/science.aax7852

Science

CRISPR-mediated live imaging of genome editing and transcription

Haifeng Wang, Muneaki Nakamura, Timothy R. Abbott, Dehua Zhao, Kaiwen Luo, Cordelia Yu, Cindy M. Nguyen, Albert Lo, Timothy P. Daley, Marie La Russa, Yanxia Liu and Lei S. Qi

Science **365** (6459), 1301-1305.
DOI: 10.1126/science.aax7852originally published online September 5, 2019

Tracking nucleic acids in living cells

Fluorescence in situ hybridization (FISH) is a powerful molecular technique for detecting nucleic acids in cells. However, it requires cell fixation and denaturation. Wang *et al.* found that CRISPR-Cas9 protects guide RNAs from degradation in cells only when bound to target DNA. Taking advantage of this target-dependent stability switch, they developed a labeling technique, named CRISPR LiveFISH, to detect DNA and RNA using fluorophore-conjugated guide RNAs with Cas9 and Cas13, respectively. CRISPR LiveFISH improves the signal-to-noise ratio, is compatible with living cells, and allows tracking real-time dynamics of genome editing, chromosome translocation, and transcription.

Science, this issue p. 1301